Elastic, thermodynamic, and electronic properties of MnSi, FeSi, and CoSi

Alla E. Petrova,[1] Vladimir N. Krasnorussky,[1] Anatoly A. Shikov,[2] William M. Yuhasz,[3] Thomas A. Lograsso,[3] Jason C. Lashley,[4] and Sergei M. Stishov[1,*]

[1]*Institute for High Pressure Physics, Russian Academy of Sciences, Troitsk, Moscow Region 142190, Russia*

[2]*Russian Research Center, Kurchatov Institute, Moscow 123182, Russia*

[3]*Ames Laboratory, Iowa State University, Ames, Iowa 50011, USA*

[4]*Los Alamos National Laboratory, Los Alamos, New Mexico 87545, USA*

(Received 4 June 2010; revised manuscript received 1 August 2010; published 18 October 2010)

Measurements of the sound velocities, heat capacities, magnetic susceptibilities, and electrical resistivities of single crystals of MnSi, FeSi, and CoSi were performed in the temperature range 2.5–300 K and the elastic constants were calculated. The temperature dependence of the mentioned quantities reveals nontrivial features, reflecting specifics of magnetic and electron subsystems in these materials.

DOI: 10.1103/PhysRevB.82.155124 PACS number(s): 62.20.de, 65.40.Ba

The intermetallic compounds MnSi, FeSi, and CoSi with a cubic B20 crystal structure of space group $P2_13$ have attracted much attention over decades due to their remarkable magnetic and electrical properties.

MnSi is an itinerant magnet with a Curie point of about 29 K. The space group $P2_13$ allows nonzero value of the Dzyaloshinski-Moria term in energy, which causes a long wave modulation of magnetic spin structure in MnSi.[1–3] Correspondingly magnetic order in MnSi was identified as a long period ferromagnetic spiral or helical spin structure with a pitch of 180 Å ($q=0.035$ Å^{-1}).[4] The magnetic phase transition in MnSi was extensively studied (see, for instance, Refs. 5–12 and literature references therein).

Nevertheless, some remarkable properties of the phase transition in MnSi are not understood. In particular, some quantities, such as thermal-expansion coefficient, heat capacity, and temperature coefficient of resistivity display well-defined anomalies on the high-temperature side of their corresponding peaks at the phase transition.[10–12] The nature of these anomalies still remains a puzzle.

FeSi, a strongly correlated semiconductor, having a small energy gap of about 0.05 eV at low temperature, reveals metallic properties above 100 K.[13–17] Angle-resolved photoemission spectroscopy demonstrates the disappearance of an energy gap in FeSi at high temperatures.[18–20] One of the intriguing features of the physical properties of FeSi is the growth of its magnetic susceptibility at temperatures above 100 K, which reaches a broad maximum at 500 K, followed by Curie-Weiss behavior at higher temperatures. Its electrical conductivity also rises steeply in the same temperature interval as the magnetic susceptibility. No magnetic ordering in FeSi has been found at any temperature.[21]

CoSi is a diamagnetic semimetal with very high residual resistivity, implying existence of a fairly large number of defects.[22] It was widely studied as a potential material for the thermoelectric applications.[22–24] Electronic properties of MnSi, FeSi, and CoSi are generally well in agreement with the band structure and density-of-state calculations (see, for instances, Refs. 25–28) though the gap closing in FeSi is not reproduced in the calculations. So a comparative study of silicides of the transition metals is important for better understanding of physics of FeSi.

Although the compounds under study display a range of properties their lattice parameters change very little, consistent with the trend in metallic radii for Mn, Fe, and Co.[29] All these facts tell us that the total energies of these substances are not sensitive to the details of their electron and magnetic structures. However, as is shown below the specifics of the macroproperties of these silicides can be observed through the second derivatives of the total energy with respect to deformation, i.e., their elastic properties.

We report here results of studies of the sound velocities, heat capacities, magnetic susceptibilities, and electrical resistivities of single crystals of MnSi, FeSi, and CoSi. Some our data for MnSi have been already published in Refs. 10–12. They are partly reproduced here for the comparison purpose. The single crystals were grown by the Bridgman (MnSi, CoSi) and the Czochralski (FeSi) methods. The lattice parameters of the crystals, determined by x-ray diffraction, correspond well to literature values (see Table I). Electron-probe microanalysis showed some deviations from the stoichiometric chemical compositions (Table I), which are common to the silicide compounds. Note that the deviations from stoichiometry grow with a number of the valence states in the row: CoSi-FeSi-MnSi.

For further characterization of the crystals, electrical resistivity, magnetic susceptibility, and heat capacity were measured. Electrical measurements were made by a four terminal dc method. Magnetic susceptibilities were measured with a Quantum Design magnetic properties measurement system. Heat capacity was measured with adiabatic vacuum calorimeter by the heat-pulse method. A linear thermal-

TABLE I. Lattice parameters (a) and chemical compositions of MnSi, FeSi, and CoSi.

	a [a] (Å)	a [b] (Å)	Metal (at. %)	Si (at. %)
MnSi	4.5598(2)	4.558(2) (Ref. 30)	50.63	49.37
		4.5559(3) (Ref. 31)		
FeSi	4.4827(1)	4.485(1) (Ref. 32)	50.16	49.84
		4.48798(9) (Ref. 33)		
CoSi	4.444(1)	4.438 (Ref. 34)	50.07	49.93
	4.4438(6)	4.43 (Ref. 35)		

[a]Current work.

[b]Literature data.

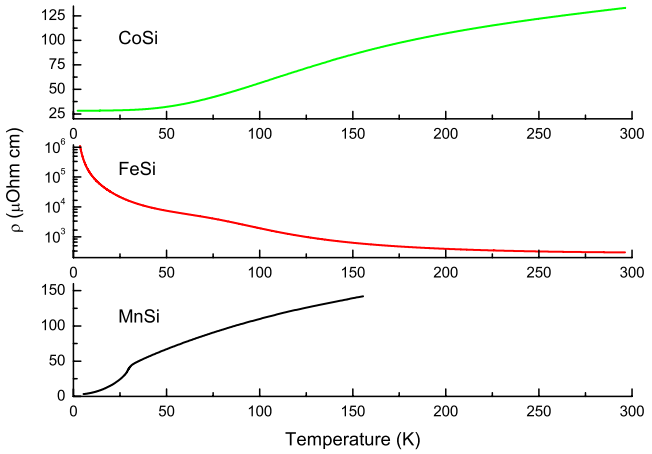

FIG. 1. (Color online) Temperature dependence of resistivity of MnSi, FeSi, and CoSi.

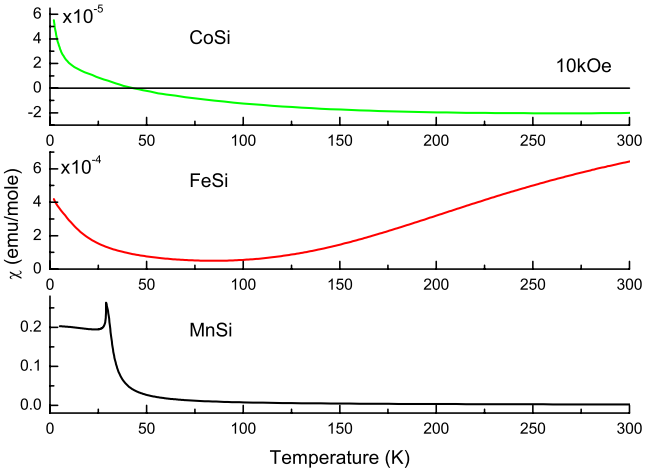

FIG. 3. (Color online) Magnetic susceptibilities of MnSi, FeSi, and CoSi as functions of temperature.

expansion measurement of CoSi was performed in a capacitance dilatometer with resolution about 0.05 Å. Figures 1–6 and 12. display results of the corresponding measurements. Temperature dependence of electrical resistivities of MnSi, FeSi, and CoSi is shown in Fig. 1. As is seen the resistivity curve of MnSi reveals existence of the magnetic phase transition at ~29 K and a saturation tendency at high temperatures. The residual resistivity is about 2 $\mu\Omega$ cm, leading to the residual resistance ratio (RRR) ~100. The resistivity of FeSi demonstrates a complex behavior, which includes three different regimes. Figure 2(a) shows that in the temperature regime below about 100 K the resistivity can be approximated by the expression for variable range hopping. In the narrow temperature region of 100–150 K, the resistivity can be described by a standard activation formula with an energy gap E_g of 0.06 eV or 690 K [Fig. 2(b)]. Close to room temperature the resistivity crosses over into a saturation regime, which seems to be too early for a semiconductor with the indicated gap. That probably signifies the gap closing and entry into a metallic state in agreement with Refs. 18–20. All these observations generally agree with literature data (see, for instance, Ref. 17).

The CoSi resistivity curve behaves like ones of high resistivity alloys with a residual resistivity of ~30 $\mu\Omega$ cm and the RRR ~4.5 (Fig. 1). The magnetic susceptibilities of the compounds as functions of temperature are shown in Fig. 3. The MnSi susceptibility curve is characterized by the sharp peak at the magnetic phase transition and the Curie-Weiss-type behavior at $T > T_c$ (see Refs. 10 and 11). The magnetic susceptibility of FeSi passes through a minimum at T ~80 K, indicating the existence of an impurity or defect—induced local magnetic moments at low temperatures and the high temperature increase in the susceptibility still of controversial nature.[13–16] CoSi is diamagnetic over a wide range of temperatures but displays a paramagnetic behavior at $T <$ ~50 K. Magnetization of CoSi at two selected temperatures is depicted in Fig. 4. These data agree well with findings of Ref. 36 but contradict to the results of Ref. 37, where a temperature-independent diamagnetic susceptibility was found in a broad range of temperature. In this connection it is worth noting that the silicides are always slightly off stoichiometric (see, for instance, Table I) and, hence, contain structural defects serving as traps for electrical carriers at low temperature with corresponding consequences for the magnetic susceptibility.

The heat capacity divided by temperature (C_p/T) for MnSi, FeSi, and CoSi is shown in Fig. 5. The prominent anomaly of C_p/T with the sharp peak on top of it signifies the magnetic phase transition in MnSi.[10] Extrapolation of C_p/T for MnSi to zero temperature gives an extremely large

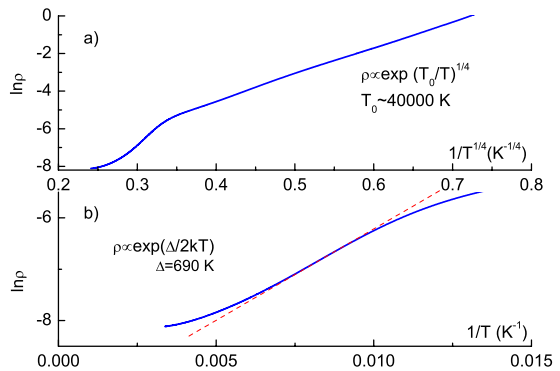

FIG. 2. (Color online) Electrical resistivity on a logarithmic scale as a function of $T^{-1/4}$ and T^{-1} for FeSi.

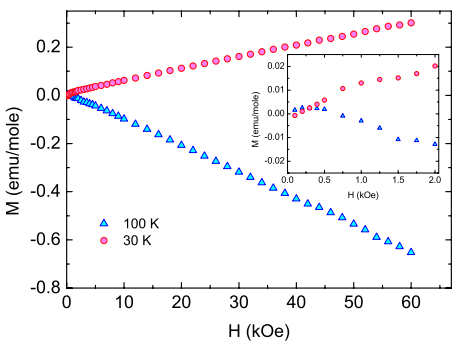

FIG. 4. (Color online) Magnetization of CoSi at T=30 and 100 K.

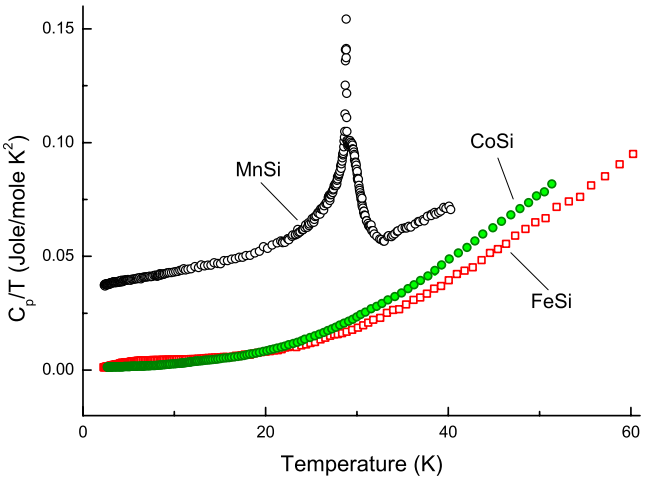

FIG. 5. (Color online) Specific heats of MnSi, FeSi, and CoSi divided by temperature.

value of the Sommerfeld constant $\gamma=36$ mJ/mol K^2, which defines a magnitude of the electron contribution to the heat capacity.[11] Behavior of C_p/T for FeSi and CoSi looks quite simple at Fig. 5, though in reality it is not true in case of FeSi at low temperatures.

The heat capacity C_p of FeSi was described in Ref. 16 in the temperature range 0.2–10 K as a combination of the common low-temperature electronic and lattice contributions and two Schottky anomalies. Surprisingly, a value of $\gamma=1.1$ mJ/mol K^2, obtained in Ref. 16, was close to the those typical of simple metals. However, on the basis of the current experiments, we could not confirm the conclusion of a finite value C_p/T at $T=0$ for FeSi. On the other hand the heat capacity of CoSi undoubtedly contains a linear temperature term γT with $\gamma \sim 1.2$ mJ/mol K^2 (Fig. 6).

The sound-velocity measurements were performed using a digital pulse-echo technique (see details in Ref. 12) in the temperature range 4–300 K (4–150 K for MnSi). Samples of MnSi, FeSi, and CoSi of about 2–4 mm thicknesses and with orientations along [100], [110], and [111] were cut from big

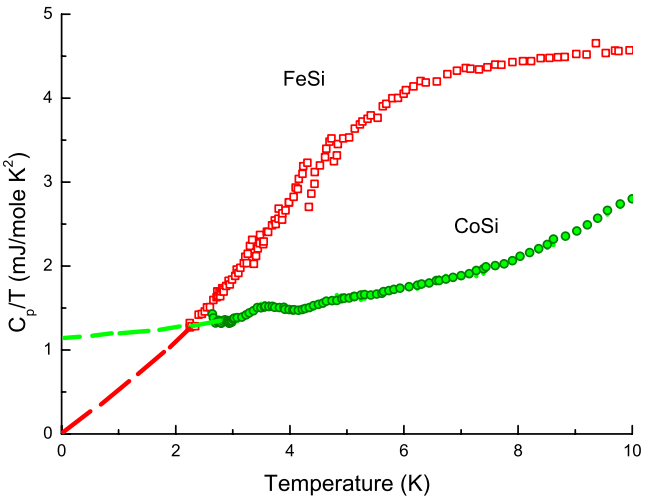

FIG. 6. (Color online) Specific heats of FeSi and CoSi divided by temperature (enlarged view of the low-temperature parts).

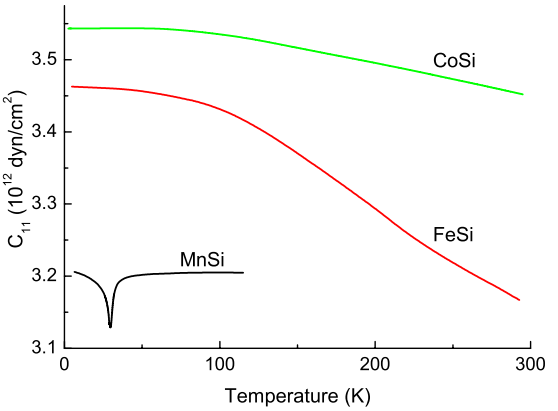

FIG. 7. (Color online) Elastic constants c_{11} of MnSi, FeSi, and CoSi.

single crystals. The corresponding surfaces of the samples were made optically flat and parallel. The 36° Y (*P*-wave) and 41° X (*S*-wave) transducers were bonded to the samples with various adhesives, including silicon greases and superglue. Temperature was measured by a calibrated Cernox sensor with an accuracy of 0.02 K.

The speed of sound and elastic constants are calculated using the known thickness and density of the samples and the relationship $c_{ij}=\rho V^2$. The precision of the sound-velocity measurements is about 0.1%, though the absolute accuracy may be of order 1% mainly due to uncertainty connected with a phase shift at the transducers sample bond interface. Results of the measurements and calculations are shown in Figs. 7–11 and Table II. Low-resolution ultrasonic data for a number of silicides of transition metals were published in Ref. 38. The temperature dependence of the elastic moduli of FeSi was measured previously using the resonant ultrasound spectroscopy technique.[39] The data from Ref. 39 generally agrees with our results where they overlap at temperatures ($T>77$ K), although some differences in temperature calibration are present.

Now we turn to the analysis of the current data on elastic properties of MnSi, FeSi, and CoSi. As is seen from Figs. 7 and 8, the values of c_{11} and c_{12} elastic constants in the row MnSi-FeSi-CoSi change according to positions of the metal-

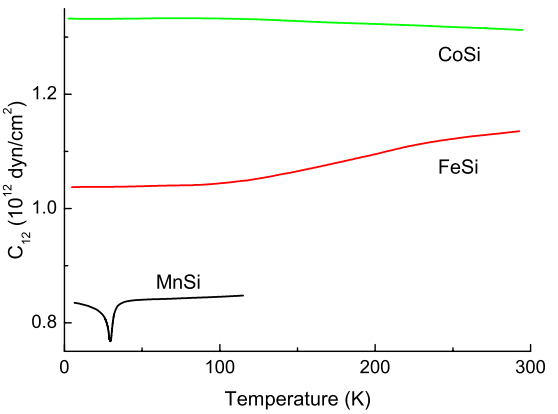

FIG. 8. (Color online) Elastic constants c_{12} of MnSi, FeSi, and CoSi.

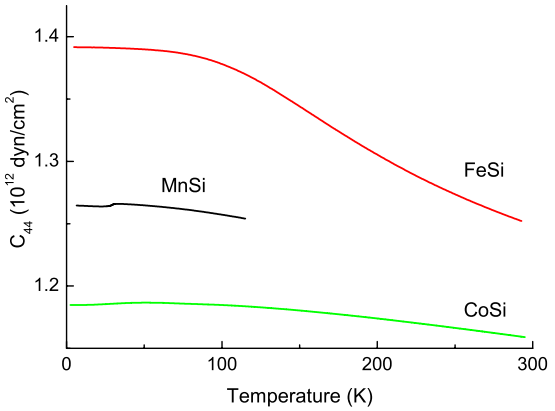

FIG. 9. (Color online) Elastic constants c_{44} of MnSi, FeSi, and CoSi.

lic atoms in the Mendeleev periodic table or, in the other words, according to the number of $3d$ valence electrons in these compounds. A slight difference in this characteristic of the materials evidently result in subtle variation in the cohesion energies and lattice parameters, though that caused quite observable difference in the elastic constants. It needs to be emphasized that the mentioned regularity exists despite the specifics of electron and magnetic structures of the compounds. Indeed it is instructive to look at the situation at low temperatures where CoSi is a semimetal with a good metallic value of the Sommerfeld constant, FeSi is a narrow gap semiconductor, and MnSi is an almost heavy fermion metal with the helical magnetic structure. The values of c_{11} and c_{12} elastic constants are highest for CoSi, then follow FeSi and MnSi (Figs. 7 and 8).

The situation is different in case of the shear elastic constants c_{44} (Fig. 9) and shear moduli $(c_{11}-c_{12})/2$ (Fig. 10) where FeSi has now the highest value and CoSi the smallest. It seems quite natural that CoSi with the highest electron concentration, has the highest bulk modulus $K=(c_{11}+2c_{12})/3$. At the same time, it is not quite clear why CoSi should have the smallest shear moduli c_{44} and $(c_{11}-c_{12})/2$ (Figs. 9 and 10). The temperature variations in the elastic properties of the three compounds are far from triviality. Though in the case of CoSi there are no significant features to be seen on the scale of Figs. 7–10. However, if we look

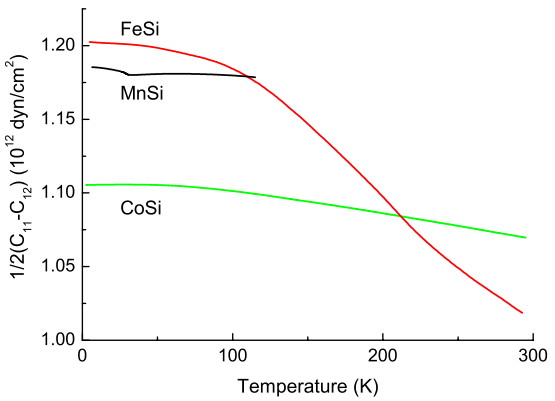

FIG. 10. (Color online) Shear moduli $(c_{11}-c_{12})/2$ of MnSi, FeSi, and CoSi.

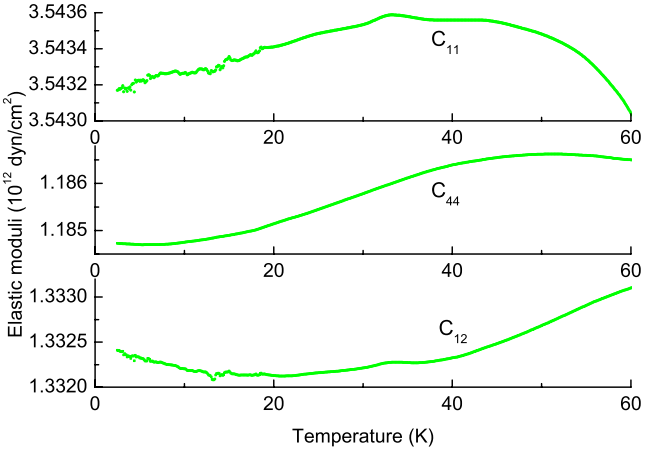

FIG. 11. (Color online) Elastic constants of CoSi (enlarged view).

closely at the temperature dependence of CoSi below 60 K (Fig. 11), we can clearly see an unusual softening of the elastic constants.

The elastic constants c_{11} and c_{44} of FeSi strongly decrease at high temperature as compared with CoSi; whereas c_{12} grows anomalously over the entire range of temperature. As a consequence the shear modulus $(c_{11}-c_{12})/2$ of FeSi drops off precipitously above 100 K (Fig. 10). This behavior is consistent with the energy gap closing as indicated in Refs. 18–20. The MnSi elastic constants that control propagation of longitudinal waves reveal significant softening at $\sim$30 K and small discontinuities at 28.8 K, which corresponds to the magnetic phase transition in MnSi. In contrast, the shear elastic moduli, do not show any softening and only respond to small volume deformations caused by the magnetovolume effect.[11]

Returning to CoSi we are reminded that temperature derivatives of physical quantities level off at low temperatures and tend to zero at $T\rightarrow 0$. As seen in Figs. 7–10, this seems to occur at about $T/\Theta_D \approx 1/6$, where Θ_D is the Debye tem-

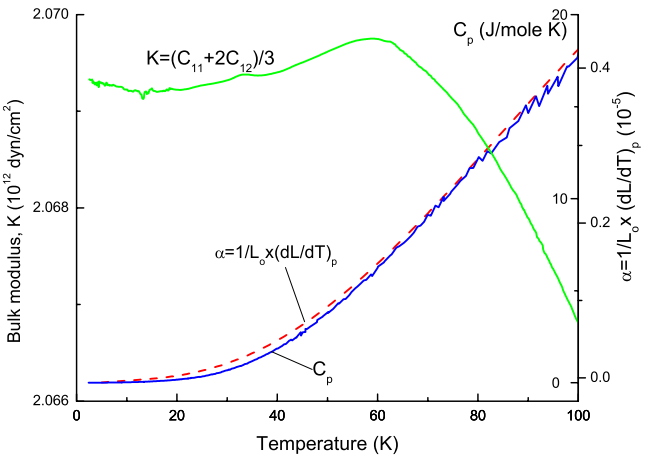

FIG. 12. (Color online) Bulk modulus, heat capacity, and coefficient of thermal expansion of CoSi. Note that the only ultrasound measurements are sensitive enough to see peculiar properties of CoSi.

TABLE II. Elastic constants of MnSi, FeSi, and CoSi (a—lattice parameters, Θ_D—Debye temperature, calculated from elastic constants).

	MnSi a=4.5598 Å, Θ_D=660 K		
c_{ij}	T=6.5	T=78	T=115
c_{11}	3.2057	3.2045	3.2047
c_{44}	1.2615	1.2582	1.2540
c_{12}	0.8523	0.8574	0.8477
	FeSi a=4.483 Å, Θ_D=680 K		
c_{ij}	T=6.5	T=77.8	T=292.8
c_{11}	3.4626	3.4454	3.1670
c_{44}	1.3916	1.3858	1.2521
c_{12}	1.0576	1.0608	1.1298
	CoSi a=4.444 Å, Θ_D=625 K		
c_{ij}	T=6.5	T=77.8	T=292.8
c_{11}	3.5432	3.5404	3.4529
c_{44}	1.1847	1.1857	1.1593
c_{12}	1.3323	1.3331	1.3128

perature. But this is not always the case as indicated by the temperature dependence of the CoSi elastic constants featured in Fig. 11 (see also Fig. 12). One can see that with decreasing temperature the elastic constants of CoSi unexpectedly pass through maxima between 40 and 70 K and continue to change down to 2.5 K. This may be tied to the Curie-Weiss-type increase in the magnetic susceptibility of CoSi below ~50 K, associated with local moment formation (see Figs. 3 and 4). The origin of these moments is probably connected with conduction electron localization at lattice defects that in turn renormalize the phonon spectra of CoSi. A concept of the "electronic glass" may be applicable to this case.

Clearly, this is not a complete explanation considering that FeSi, which also features a Curie-Weiss tail, does not display any irregularities in the elastic constants. Along with this unexplained behavior, the description of the elastic properties of CoSi cannot be done based on a single energy-scale like the Debye temperature. Rather an entire spectrum of characteristic energies down to ~1 K may be required.

In summary, we have measured the resistivity, magnetic susceptibility, heat capacity, and sound velocities in MnSi, FeSi, and CoSi. All the measured properties of MnSi display distinct imprints of the magnetic phase transitions at 29 K. The temperature dependence of resistivity and magnetic susceptibility of FeSi correlate with the anomalous softening of c_{11} and c_{44} and hardening of c_{12} elastic constants at about 100 K, as compared with the regular behavior of CoSi, which agrees with the observation of gap closing in FeSi. The regularity in behavior of the elastic constants of CoSi appears to be illusive. They continue to change down to the lowest temperature (~2.5 K) seemingly indicates a glasslike behavior.

We express our deep gratitude to Joe Thompson for the technical assistance. A.E.P., S.M.S., and V.N.K. appreciate support of the Russian Foundation for Basic Research, Program of the Physics Department of RAS on Strongly Correlated Systems, and Program of the Presidium of RAS on Physics of Strongly Compressed Matter. W.M.Y. and T.A.L. wish to acknowledge research performed at Ames Laboratory. Ames Laboratory is operated for the U.S. Department of Energy by Iowa State University under Contract No. DE-AC02–07CH11358. Work at Los Alamos was performed under the auspices of the U.S. Department of Energy, Office of Science.

*sergei@hppi.troitsk.ru

[1] H. J. Williams, J. H. Wernick, R. C. Sherwood, and G. K. Wertheim, J. Appl. Phys. **37**, 1256 (1966).
[2] I. Dzyaloshinsky, J. Phys. Chem. Solids **4**, 241 (1958).
[3] T. Moriya, Phys. Rev. **120**, 91 (1960).
[4] Y. Ishikawa, K. Tajima, D. Bloch, and M. Roth, Solid State Commun. **19**, 525 (1976).
[5] J. D. Thompson, Z. Fisk, and G. G. Lonzarich, Physica B **161**, 317 (1989).
[6] C. Pfleiderer, G. J. McMullan, S. R. Julian, and G. G. Lonzarich, Phys. Rev. B **55**, 8330 (1997).
[7] C. Thessieu, J. Flouquet, G. Lapertot, A. N. Stepanov, and D. Jaccard, Solid State Commun. **95**, 707 (1995).
[8] C. Thessieu, Y. Kitaoka, and K. Asayama, Physica B **259-261**, 847 (1999).
[9] K. Koyama, T. Goto, T. Kanomata, and R. Note, Phys. Rev. B **62**, 986 (2000).
[10] S. M. Stishov, A. E. Petrova, S. Khasanov, G. Kh. Panova, A. A. Shikov, J. C. Lashley, D. Wu, and T. A. Lograsso, Phys. Rev. B **76**, 052405 (2007).
[11] S. M. Stishov, A. E. Petrova, S. Khasanov, G. Kh. Panova, A. A. Shikov, J. C. Lashley, D. Wu, and T. A. Lograsso, J. Phys.: Condens. Matter **20**, 235222 (2008).
[12] A. E. Petrova and S. M. Stishov, J. Phys.: Condens. Matter **21**, 196001 (2009).
[13] V. Jaccarino, G. K. Wertheim, J. H. Wernick, L. R. Walker, and S. Arajs, Phys. Rev. **160**, 476 (1967).
[14] Z. Schlesinger, Z. Fisk, H.-T. Zhang, M. B. Maple, J. F. DiTusa, and G. Aeppli, Phys. Rev. Lett. **71**, 1748 (1993).
[15] D. Mandrus, J. L. Sarrao, A. Migliori, J. D. Thompson, and Z. Fisk, Phys. Rev. B **51**, 4763 (1995).
[16] S. Paschen, E. Felder, M. A. Chernikov, L. Degiorgi, H. Schwer, H. R. Ott, D. P. Young, J. L. Sarrao, and Z. Fisk, Phys. Rev. B **56**, 12916 (1997).
[17] M. Fäth, J. Aarts, A. A. Menovsky, G. J. Nieuwenhuys, and J. A. Mydosh, Phys. Rev. B **58**, 15483 (1998).
[18] K. Ishizaka, T. Kiss, T. Shimojima, T. Yokoya, T. Togashi, S. Watanabe, C. Q. Zhang, C. T. Chen, Y. Onose, Y. Tokura, and S.

Shin, Phys. Rev. B **72**, 233202 (2005).
[19] M. Arita, K. Shimada, Y. Takeda, M. Nakatake, H. Namatame, M. Taniguchi, H. Negishi, T. Oguchi, T. Saitoh, A. Fujimori, and T. Kanomata, Phys. Rev. B **77**, 205117 (2008).
[20] M. Klein, D. Zur, D. Menzel, J. Schoenes, K. Doll, J. Röder, and F. Reinert, Phys. Rev. Lett. **101**, 046406 (2008).
[21] K. Tajima, Y. Endoh, J. E. Fischer, and G. Shirane, Phys. Rev. B **38**, 6954 (1988).
[22] C. S. Lue, Y. K. Kuo, C. L. Huang, and W. J. Lai, Phys. Rev. B **69**, 125111 (2004).
[23] S. Asanabe, D. Shinoda, and Y. Sasaki, Phys. Rev. **134**, A774 (1964).
[24] A. Sakai, F. Ishhii, Y. Onose, Y. Tomioka, S. Yotsuhashi, H. Adachi, N. Nagaosa, and Y. Tokura, J. Phys. Soc. Jpn. **76**, 093601 (2007).
[25] O. Nakanishi, A. Yanase, and A. Hasegawa, J. Magn. Magn. Mater. **15-18**, 879 (1980).
[26] L. F. Mattheiss and D. R. Hamann, Phys. Rev. B **47**, 13114 (1993).
[27] Y. Imai, M. Mukaida, K. Kobayashi, and T. Tsunoda, Intermetallics **9**, 261 (2001).
[28] J. Guevara, V. Vildosola, J. Milano, and A. M. Llois, Phys. Rev. B **69**, 184422 (2004).
[29] W. A. Harrison, *Elementary Electronic Structure* (World Scientific, Singapore, 1999).
[30] B. Lebech, J. Bernhard, and T. Freltoft, J. Phys.: Condens. Matter **1**, 6105 (1989).
[31] J.-E. Jorgensen and S. E. Rasmussen, Powder Diffr. **6**, 194 (1991).
[32] B. C. Sales, E. C. Jones, B. C. Chakoumakos, J. A. Fernandez-Baca, H. E. Harmon, J. W. Sharp, and E. H. Volckmann, Phys. Rev. B **50**, 8207 (1994).
[33] W. Wong-Ng, H. McMurdie, B. Paretzkin, C. Hubbard, and A. Dragoo, Powder Diffr. **2**, 261 (1987).
[34] B. Boren, Ark. Kemi, Mineral. Geol. **11**, 1 (1933).
[35] Hadfields Limited, Sheffield, England, UK (private communication).
[36] A. Amamou, P. Bach, F. Gautler, C. Robert, and J. Castaing, J. Phys. Chem. Solids **33**, 1697 (1972).
[37] J. H. Wernick, G. K. Wertheim, and R. C. Sherwood, Mater. Res. Bull. **7**, 1431 (1972).
[38] G. P. Zinoveva, L. P. Andreeva, and P. V. Geld, Phys. Status Solidi A **23**, 711 (1974).
[39] J. L. Sarrao, D. Mandrus, A. Migliori, Z. Fisk, and E. Bucher, Physica B **199-200**, 478 (1994).